Poststall/Spin Characteristics of an LK-10A Sailplane

Donald T. Ward*
Air Force Flight Test Center, Edwards Air Force Base, Calif.
A. George Bennett† and John K. Owens‡
Mississippi State University, Mississippi State, Miss.

The post-stall and spin characteristics of a Laister-Kaufmann LK-10A sailplane were explored. The sailplane was instrumented to measure angular rates, linear accelerations, angle of attack, sideslip angle, airspeed, altitude, and control surface positions. The spin characteristics of the sailplane were investigated at 1%, 36%, 49%, and 99% of the allowable center of gravity range. Developed spins could not be attained for the 1% and 36% center of gravity positions. Developed spins were attained at the 49% cg position when the elevator deflection limit was increased from 15° to 25°. The LK-10A sailplane exhibited two mildly oscillatory spin modes when flown at the 99% aft cg position. The average angles of attack for these two spin modes were approximately 30° and 55°, respectively. Maximum instantaneous angles of attack of 70° were attained.

Nomenclature

cg	= center of gravity
$n_{z_{cg}}$	= normal acceleration at aircraft cg
p	= body-axis roll rate
q	= body-axis pitch rate
r	= body-axis roll rate
α	= body-axis angle of attack
β	= sideslip angle
δ_a	= aileron surface deflection
δ_e	= elevator surface deflection
δ_r	= rudder surface deflection

Subscripts

avg	= average
max	= maximum
s	= stall
trim	= trimmed value

Introduction

THE quantitative flight testing of sailplanes has been limited primarily to performance measurements to determine sink rate vs airspeed. This testing technique is highly developed as reported by Bikle,[1-7] Zacher,[8,9] and Johnson.[10] Whitfield[11] has developed an automatic method to record airspeed and altitude necessary for the gliding performance evaluation. Performance flight testing is presently limited only by the ability to determine atmospheric motions. Most flight testing of sailplanes to establish stability and control characteristics has consisted of qualitative pilot evaluations. Paiewonsky[12,13] reviewed the theoretical longitudinal and lateral stability and control requirements for the sailplane and later outlined a flight test program[14] to quantitatively measure the response of sailplanes to establish a correlation between theory and experiment. Recently, Trode[15] has conducted flight test measurements of the longitudinal stability and control parameters of a fiberglass sailplane and found significant degradation in the stick fixed stability due to fuselage elasticity.

Presented as Paper 74-1023 at the AIAA/MIT/SSA 2nd International Symposium on the Technology and Science of Low Speed and Motorless Flight, Cambridge, Mass., September 11-13, 1974. Submitted September 27, 1974; revision received October 28, 1975. This work was supported in part by the Air Force Flight Dynamics Laboratory under contract F33615-72-C-119.

Index category: Aircraft Testing (including Component Wind Tunnel Testing).

*Director, F-15 Joint Test Force. Colonel, U.S. Air Force. Member AIAA.

†Associate Professor of Aerospace Engineering, Member AIAA.

‡Assistant Professor of Electrical Engineering.

Since 1949 the Raspet Flight Research laboratory (RFRL) of Mississippi State University (MSU) has utilized the sailplane to study many of the problems of low-speed flight. In mid-1971 a flight test program to investigate the feasibility of using the sailplane as a post-stall research vehicle was conducted under the auspices of the Flight Control Division, Air Force Flight Dynamics Laboratory (AFFDL). The sailplane was a very attractive vehicle for post-stall research for several reasons: (1) it has no power effects; (2) fully developed flat spins have been reported for several configurations, particularly with aft cg loadings; (3) adequate payload capacity is available for instrumentation; (4) structural modifications are relatively easy to make; and (5) direct operating costs are low.

The objectives of the study were to modify the Laister-Kaufmann LK-10A sailplane with appropriate instrumentation and an anti-spin parachute, to flight-qualify the anti-spin parachute, and to determine the spin characteristics of the basic sailplane. To quantify the motions of the sailplane during the post-stall maneuvers, three axis inertial sensors and wind axis sensors were required. Their outputs were recorded onto magnetic tape for later data manipulation to compute angle of attack, sideslip angle, and accelerations at the sailplane cg. A total of 27 flights were made to determine the spin envelope of the basic LK-10A configuration. An average of three spin maneuvers and three low angle of attack maneuvers were made during each flight. The effects of cg position, elevator angle and lateral-directional control inputs upon the spin characteristics were evaluated.

Sailplane Description, Modifications, and Instrumentation

Sailplane Description

The test vehicle was a Laister-Kaufmann LK-10A sailplane originally manufactured in 1942 and converted to the so-called "flat-top" configuration in 1950 by Dr. August Raspet's team at MSU. Figures 1 and 2 show the sailplane used for the flight tests, and its basic dimensions are given in Table 1.

This sailplane was chosen for four basic reasons. First, RFRL had two such aircraft available for use: one which was used for pilot checkout and proficiency, and the test aircraft. The LK-10A also has a reputation for structural soundness and reliability.[16] The steel tube fuselage truss could be modified easily to accept the loads imposed by the anti-spin parachute. Finally, since the LK-10A is a two-place sailplane, a 150-pound payload capacity and ample volume in the rear cockpit to accomodate the instrumentation system were available.

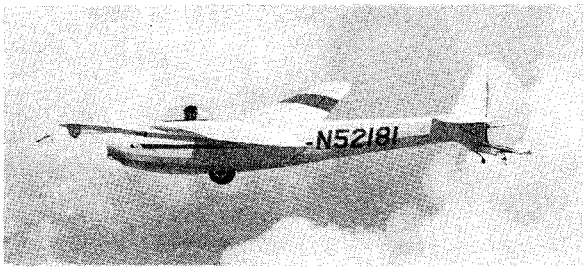

Fig. 1 LK-10A sailplane.

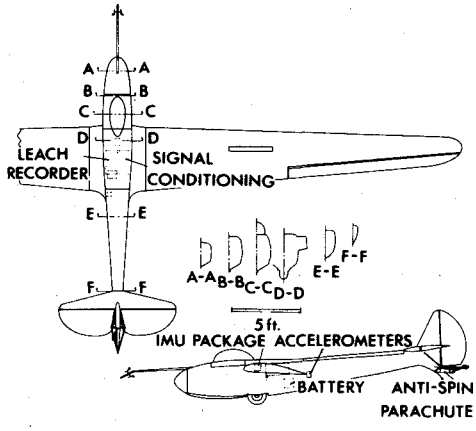

Fig. 2 Three-view layout of LK-10A sailplane and instrumentation.

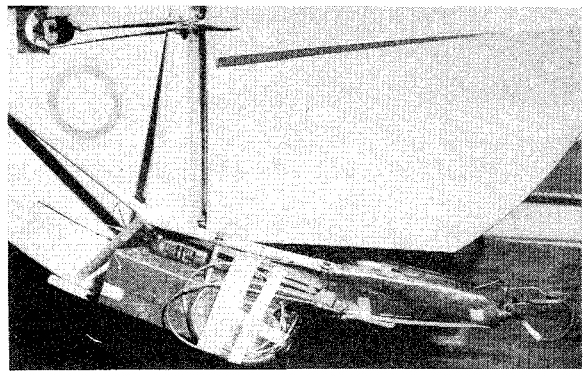

Fig. 3 Anti-spin parachute installation.

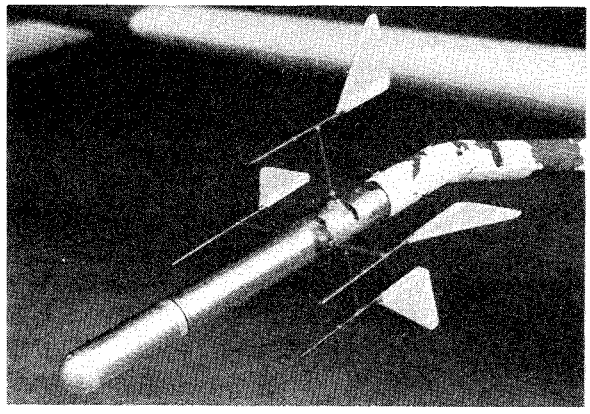

Fig. 4 Airspeed, angle of attack, and sideslip angle probe.

Modifications

Major modifications to the LK-10A included the addition of a ballistically-deployed anti-spin parachute, aft fuselage longeron doublers to withstand the anticipated parachute loads, and an instrumentation system capable of sensing and recording 17 channels of data. The placement of the parachute and instrumentation is shown in Fig. 2. The anti-spin parachute was a 6-ft diameter solid canopy type originally used on the XV-11A STOL research airplane. A pyrotechnic device, actuated by a cable pull from the cockpit, propelled a slug that extracted the parachute, lines-first, out of its cannister to the full extent (approximately 15 ft) of the parachute attachment line. Thus the canopy inflated in a flowfield relatively unaffected by the separated flow around the aircraft. Figure 3 shows the complete anti-spin parachute installation.

The moments of intertia of the sailplane were experimentally determined using a spring suspension arrangement.[19] Rate gyro outputs were used to determine the period of oscillation.

Table 1 LK-10A Description

Span	50 ft
Length	21.5 ft
Height	4.6 ft
Maximum gross weight	875 lbs
Wing area	166 ft^2
Moment of inertia I_x	578 slug-ft^2
Moment of inertia I_y	435 slug-ft^2
Moment of inertia I_z	1488 slug-ft^2
Moment of inertia I_{xz}	18 slug-ft^2
Dihedral angle	4.25°
Root airfoil	NACA 4418
Tip airfoil	NACA 4409
Horizontal tail area	21.3 ft^2
Vertical tail area	13.2 ft^2
Aileron area	18.0 ft^2
Elevator travel	15° up, 25° down
Rudder travel	±27°

Instrumentation

Due to restricted funding, the onboard instrumentation package was limited to government furnished equipment and RFDL prototype electronics. A breadboard strapdown attitude system[17] was supplied by AFFDL as the inertial sensor package. This unit computed angular accelerations and Euler angles rather than using independent sensors. Unresolvable electronic difficulties finally forced RFRL to separate the inertial measuring unit (IMU) from the computing and display units and use only the IMU. Using this expedient, the basic inertial sensors were three subminiature Northrop GR-65 rate gyros and three Northrop APS-3 pendulous linear accelerometers. Calibrations determined that the rate gyro ranges were ±260°/sec, ±100°/sec, ±130°/sec for p, q, and r, respectively. No centrifuge was available for accelerometer calibrations, so the IMU accelerometer ranges could not be checked beyond ±1.0 g prior to flight. A second set of three-axis linear accelerometers (potentiometer-type Honeywell GG22B1 instruments) were installed in the aft cockpit and on the right wing spar root fitting as backups for the IMU linear accelerometers.

A combination flow direction and pitot-static sensor (FDAPS), Fig. 4, was developed at MSU for the large AOA range and calibrated in the 3×4 ft low-speed wind tunnel. AOA and slideslip angles were measured directly by the FDAPS vanes using Conrac microtorque potentiometers. Pitot-static pressure differential was measured with a Northam DP-70.15 psid variable reluctance transducer. A Statham PM-131-TC 10 psid strain gage transducer was referenced against sea level pressure for altitude measurement. Airspeed was computed using the total AOA of the probe to correct the measured pressure differential. No corrections were made for dynamic response of the vanes or flow distortion due to fuselage proximity.

Edcliff linear potentiometers were used to measure control surface deflections. A force measuring unit (strain gage type) was installed in series with the parachute attachment line to

measure parachute forces for the anti-spin parachute qualification flights.

During flight the outputs of the 17 independent sensors were recorded on a 14-channel Lockheed-Leach MTR-3200A analog-type recorder. Since the number of sensors exceeded the number of channels available on the recorder, one channel of the MTR-3200A was assigned to a Burr-Brown 10-channel multiplexer. To synchronize the multiplexed channels and the analog-to-digital conversion system, a 500 Hz clock signal, generated by a crystal oscillator was recorded on one channel of the MTR-3200A. Control logic circuits were used to switch in precision voltages at the sensor outputs for thru-system calibration of all data channels before and after each flight.

Instrumentation Deficiencies

During some spins the range of the yaw rate gyro was exceeded. Also, the IMU normal accelerometer saturated at approximately 1.4 g, rendering it virtually useless. Based on the backup linear accelerometer data, a maximum load factor of approximately 4.5 g was encountered during dive pullouts after spin recovery. The FDAPS sensors, particularly the α and β vanes, were highly unreliable. The circuits developed shorts often; and the signal-to-noise ratios were low. Vibrations and buffet, encountered near the stall and during periods of high angular accelerations, seemed to particularly degrade the AOA data. For some of the later flights a special numerical filter was required to allow processing of the AOA data. Control surface position potentiometers exhibited this same sort of intermittent behavior, but much less frequently than the AOA and slideslip sensor circuits.

Data Processing

A digital data acquisition and data reduction seemed to be advisable because of the interactions between sensors such as AOA and angular rate and to process the large volume of data acquired. With the flight test data in digital form, the computing power of the MSU UNIVAC 1106 could be used for data manipulation, filtering, and plotting. Analog flight test data was digitized using a Hewlett Packard 2114A minicomputer to control a high-speed HP 5710A A/D converter and to output data onto a 9-track Cipher magnetic tape unit. The data reduction program consisted of serveral parts. First, the A/D integer format of the sensor output was scaled back to engineering units. Then a digital filter[18] was applied to smooth the data. A 5-Hz cutoff, 6.5-Hz termination, 101-point digital filter was used for all data. A series of standard flight test calculations were made to transfer the inertial measurements to the aircraft cg. A high speed Gould electrostatic plotter was used to plot the output.

Flight Test Results

All flights were conducted with VHF radio contact between the test aircraft, a chase aircraft, and RFRL ground units. The chase aircraft, initially a Cessna 319 and later a Cessna Agwagon, also served as an excellent platform for motion picture photography of the post-stall maneuvers. The herbicide/pesticide tank access door was removed on the Agwagon and a seat and wind-screen were added for the photographer. From this vantage point, the photographer had an unobstructed view of the test aircraft as the chase pilot flew a descending spiral outside the sailplane's spin helix. The chase pilot also provided assistance to the test pilot with minimum altitude reminders, maximum turn count calls, qualititative comments, and immediate visual inspections of inflight equipment malfunctions.

Anti-Spin Parachute Qualification

The anti-spin parachute was deployed on five different flights: four times in wings-level, low angle of attack flight, and once in a fully developed spin. The first two deployments were unsuccessful, but after several minor modifications to the cannister, to the packing method, and to the slug attachment cable, two successful deployments were made at approximately 55 mph IAS. Wings-level anti-spin parachute deployments revealed that the glider/parachute combination was marginally stable in dutch roll. During the wings-level deployment flights, the pilot made turns of up to 270° with very shallow bank angles, but was unable to precisely maneuver the sailplane. However, after the parachute force load cell was removed, the parachute-induced lateral-directional oscillations were reduced and the parachute was released over the runway just prior to touchdown.

As the final step in qualification of the anti-spin parachute, it was deployed intentionally during a 20-turn spin. The spin parameters ($\alpha \approx 65°$, $p \approx -35°$/sec, and $r \approx -110°$/sec) at deployment were at the highest AOA and represented the most stable spin mode achieved. Even though pro-spin controls were maintained throughout the deployment, the anti-spin parachute positively recovered the aircraft, stopping the rotation in just over a half turn and lowering the nose smoothly.

Stall Definition

Stall was perceived by the pilot as an uncommanded nose-down pitching moment. Quantitatively, α_s was read from α time-histories as that value where q first became negative with δ_e increasing. On average, α_s was about 9°, although there was an uncertainty of approximately $\pm 1.5°$ in defining α_s, even in the best runs. On a few runs, α_s was quite different from this average value, apparently because of unusually large biases in the AOA sensor output signal.

Spin Resistance

The flat-top LK-10A proved to be highly spin resistant at forward and mid cg loadings. No spins were achieved at 1% cg and only two spins were achieved in 29 attempts at 36% and 49% cg loadings. Furthermore, to obtain even these two spins it was necessary to increase up elevator travel (with an adjustable elevator stop on the control stick) by approximately 10°. Since the LK-10A can be made spin-resistant simply by shifting the cg forward, pilots engaged in post-stall flight testing would probably find flights in the LK-10A instructive. They could qualitatively evaluate such a spin-resistant aircraft as part of their proficiency and/or recurrency training and experience for themselves the meaning of spin resistance in a controlled environment.

Post-Stall Gyrations

The post-stall gyration (PSG) was usually repeatable, although four attempted spin entries resulted in directional departures opposite to applied rudder. The typical PSG bore considerable resemblance to the PSG of at least one high performance attack aircraft. Figure 5 shows α, β, p, and r for a typical LK-10A PSG. AOA decreased below α_s 4 four times before recovery was initiated; further, α and r show a period of approximately 7 sec after some initial variability. The roll rate shows approximately the same period, although p has higher-order harmonics superimposed on the basic oscillations.

Lower AOA Spin Mode

A mildly oscillatory right spin having the AOA and slideslip characteristics shown in Fig. 6 was obtained with a mid cg and $\delta_{e_{max}}$ set at 25°. After three turns full right aileron was applied to investigate the effect of such an input. During the incipient phase of the spin (up to $t \simeq 27$ sec), the AOA varied between 18° and 56°, but then α settled down between 28° and 44°, with $\alpha_{avg} \simeq 35°$. Average AOA was still approximately 35° when the aileron input was made ($t \simeq 27$ sec), whereupon AOA decreased approximately 15°. After about one turn α again increased and oscillated periodically between 28° and 44° with a period of 7 sec. Sideslip angle oscillated about its trimmed value ($\beta_{trim} \simeq -4°$) through the spin; β was in phase with the α

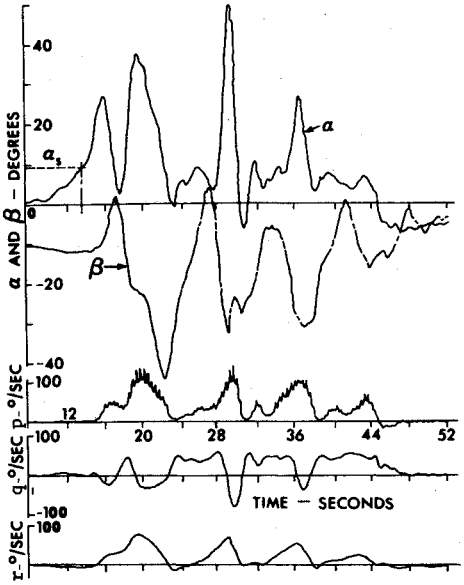

Fig. 5 Long duration post-stall gyration.

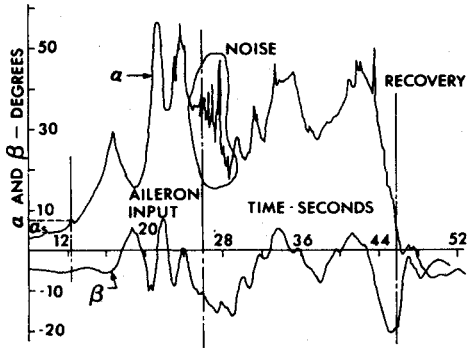

Fig. 6 AOA and sideslip in lower AOA spin mode.

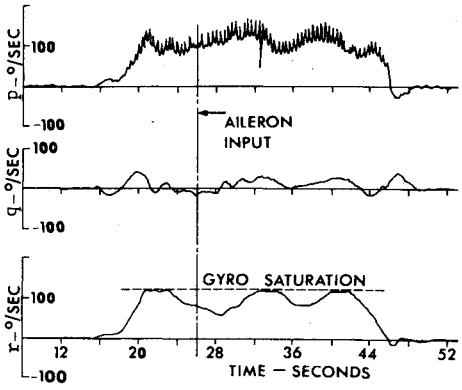

Fig. 7 Body axis angular rates in lower AOA spin mode.

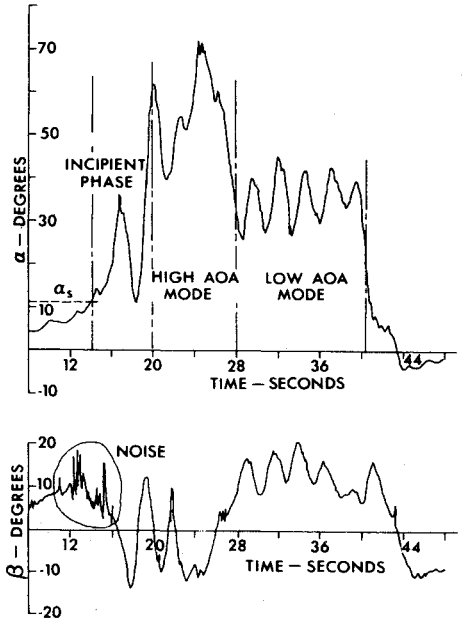

Fig. 8 AOA and sideslip in the higher AOA spin mode.

oscillations after the incipient phase ended. The most significant point is that α never decreased below approximately 17° after departure. Since α_s was about 9°, it is clear that this motion was a spin.

The body-axis angular rates for this relatively low AOA spin are shown in Fig. 7. Both p and r averaged close to 100°/sec during this maneuver and were little affected by the aileron input. However, the aircraft was initially spinning with the wing tilted slightly left wing down ($q_{avg} < 0$); as expected, the right aileron input tilted the aircraft in the opposite direction and q_{avg} became positive.

The most significant feature of Fig. 7 is to be found in the p and r traces. At roll rates greater than about 30°/sec, there is a high-frequency signal, possibly a structural vibration, superimposed on the basic aircraft motion. Obviously, this high-frequency signal results in considerable uncertainty in ascertaining the "rigid-body" roll rate of the sail plane during the spin. Digital filter weights can be adjusted to remove this oscillation frequency.

Higher AOA Spin Mode

Figure 8 shows the α and β data for a higher AOA left spin which resulted from moving the cg aft to 99% of its allowable rearward travel. This new spin mode occurred even with $\delta_{e_{max}}$ set at 15°, although air loads gave a peak elevator angle of approximately 20° during the initial stage of this higher AOA spin. This new spin mode lasted about 14 sec, roughly three and one-half turns, of which the last two turns were a partially developed phase of this mode. Apparently this motion state was unstable, since transition back to the lower AOA spin mode occurred at $t \simeq 28$ sec. The period of the lower AOA mode in this case was approximately 3.5 sec, roughly half that previously observed for α in Fig. 6.

The average AOA for the higher AOA mode was about 55°, with variations of approximately ±16°. Sideslip was mostly negative ($\beta_{avg} \simeq -4°$) during this spin mode. These data apparently suggest that yaw in the direction of rotation tended to reduce AOA, while yawing away from the direction of rotation tended to increase α.

Figure 9 shows the body-axis angular rates for the higher AOA spin mode, and r is the angular rate most affected. During this higher AOA portion of the spin, r_{avg} was approximately −90°/sec and $r_{max} \simeq -140°$/sec. After transition to the lower AOA spin mode, $r_{avg} \simeq -62°$/sec with oscillations of ±8°/sec about the mean. A higher frequency signal (approximately 2.5 Hz in this case) shows up again in

Table 2 Direct operating cost comparison

Test aircraft type	Appropriate cost/hour[a] ($)
LK-10A (with Stearman tow aircraft, Cessna Agwagon Chase aircraft)	95
T-33 (T-33A test aircraft, T-33A chase aircraft)	1,225
F-4E (F-4E test aircraft, T-38 chase aircraft)	3,525
A-7 (A-7 test aircraft, T-38 chase aircraft)	2,240
T-38 (T-38 test aircraft, T-38 chase aircraft)	1,685

[a] Cost is based on flight time of the test aircraft.

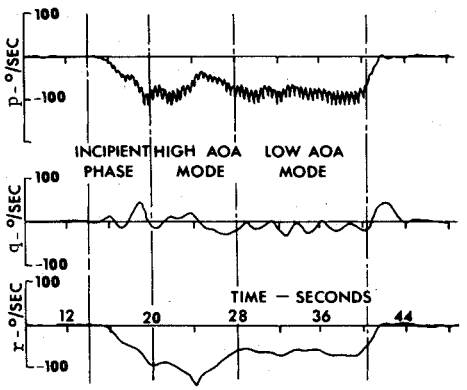

Fig. 9 Body axis angular rates in the higher AOA spin mode.

the p trace. However, p decreased noticeably as r increased; for example, when $t=24$ sec, $p\simeq -40°$/sec and $r\simeq -140°$/sec. The q trace indicated a slight wing tilt (left wing down) in the direction of rotation during the higher AOA mode; then, as the maneuver progressed toward the lower AOA mode, the right wing tilted down and q became slightly negative ($q_{avg}\simeq -2°$/sec).

The appearance of this higher AOA spin mode at aft cg and $\delta_{e_{max}}\simeq 15°$ raised hope that even higher AOA could be achieved with increased $\delta_{e_{max}}$ and/or δ_a in the direction of spin rotation. However, neither of these control inputs produced any significant changes in the character of LK-10A spins.

Recovery Characteristics

The LK-10A was easy to recover from every PSG and spin encountered using aerodynamic controls alone. The standard spin recovery procedure of full rudder opposite to spin direction, followed momentarily by easing the stick forward approximately to its neutral position, was the optimum recovery technique. Recovery ordinarily took less than one turn and about 300 ft of altitude after initiation of recovery controls. Forward stick appeared to be the most effective recovery control for the loadings tested. The aircraft would not recover when the controls were released in a spin; instead the control surfaces floated to full up elevator, full rudder in the direction of rotation, and full aileron in the direction of rotation. The aircraft showed no tendency to recover through two full turns with the control surfaces free to float to these positions.

Operating Costs

The operating costs of the LK-10A were low in comparison to jet aircraft. Table 2 summarizes the direct operating costs of the LK-10A, the tow plane, and the chase aircraft in comparison to approximate operating costs for several jet aircraft. No charges have been included for the ground crews or the pilots required by any of the systems since the comparative costs were based on USAF bailment fees with no crews provided for either the chase aircraft or the test aircraft. Even compared to the T-33, one of the least expensive jets operated by the military services, the LK-10A costs about 10% as much as the T-33 to operate.

In addition, the modifications to jet aircraft are usually quite expensive; that is, the design of the emergency spin recovery device suitable for the configuration, the resulting structural modifications to the airframe, and the flight qualification of this emergency spin recovery device can be a major cost addition. For example, approximately one million dollars were spent in modifying the F-4E spin test aircraft for the last series of post-stall tests on that aircraft.

Summary and Conclusions

The post-stall characteristics of the LK-10A were generally satisfactory for post-stall research, although developed spins were readily achieved only with an aft center of gravity. The departure was generally repeatable, although directional divergences opposite to applied rudder occurred on four occasions. The post-stall gyration of the LK-10A was milder than those usually associated with fighter-type aircraft, but the motion parameters were sufficiently disorienting to provide valuable experience for pilots training for post-stall test programs. Two mildly oscillatory spin modes were observed. The steep mode had an average angle of attack of approximately 35°, while the flatter spin mode had an average angle of attack of approximately 55°. Aerodynamic controls were always effective for recovery from all spins and post-stall gyrations, although the anti-spin parachute was satisfactorily demonstrated in one long duration spin.

The direct operating costs of the sailplane are approximately an order of magnitude less than those of operational jet aircraft normally used to explore the post-stall regime. Furthermore, the structural and system simplicity of the sailplane allows modifications to be made economically. The low cost, demonstrated safety, and broad spectrum of available post-stall motions suggests a significant post-stall research capability and a useful post-stall training potential for the sailplane.

References

[1] Bikle, P.F., "Polars of Eight," *Soaring*, Vol. 34, June 1970, p. 16.

[2] Bikle, P.F., "Gear Up, Sun Up," *Soaring*, Vol. 34, July 1970, p. 25.

[3] Bikle, P.F., "T-6 Performance," *Soaring*, Vol. 34, Oct. 1970, p. 18.

[4] Bikle, P.F., "ASW-12 and Libelle Performance Tests," *Soaring*, Vol. 34, Nov. 1970, p. 26.

[5] Bikle, P.F., "Airspeed Calibration," *Soaring*, Vol. 35, Jan. 1971, p. 22.

[6] Bikle, P.F., "Performance Summary," *Soaring*, Vol. 35, Feb. 1971, p. 18.

[7] Bikle, P.F., "Polars of Eight-1971", *Soaring*, Vol. 35, June 1971, p. 20.

[8] Morklein, H.J. and Zacher, H., "Flight Performance Measurements of Sailplanes," *Soaring*, Vol. 29, Jan. 1965, p. 8.

[9] Zacher, H., "Flight Measurements with Standard Class Sailplanes," *Soaring*, Vol. 32, Dec. 1968, p. 22.

[10] Johnson, R.H., "Sailplane Performance Measurements," *Soaring*, Vol. 32, April 1968, p. 10.

[11] Whitfield, G.R., "Glider Performance Testing with an Automatic Recording System," *Proceedings of First International Symposium on the Technology and Science of Motorless Flight*, NASA CR-2315, Oct. 1972.

[12] Paiewonsky, B., "The Handling Characteristics of Sailplanes – Part I," *Soaring*, Vol. 25, Jan. 1961, p. 6.

[13] Paiewonsky, B., "The Handling Characteristics of Sailplanes – Part II," *Soaring*, Vol. 25, Feb. 1961, p. 10.

[14] Paiewonsky, B., "A Flight Test Program for Examining Sailplane Lateral-Directional Stability and Control," *Soaring*, Vol. 33, Feb. 1969, p. 22.

[15] Torode, H.A., "Flight Evaluation of Aeroelastic Distortion Effects on Performance, Stability and Control of Sailplanes," *Proceedings of First Symposium on the Technology and Science of Motorless Flight*, NASA CR-2315, Oct. 1972.

[16] MacNicol, Allen, "Old LK's Never Die...They Just Get Modified and Modified and Modified," *Soaring*, Vol. 30, July 1966, p. 13.

[17] DeRuyck, A.R., "A Flightworthy Breadboard System for Computing Stability Attitude, and Heading from Body-Mounted Sensors," Air Force Flight Dynamics Laboratory, Wright-Patterson Air Force Base, Ohio, AFFDL-TR-71-130, Oct. 1971.

[18] Graham, R.J., "Determination and Analysis of Smoothing Weights," NASA TR-179, Dec. 1969.

[19] Boucher, Robert W. and others. "A Method for Measuring the Product of Inertia and the Inclination of the Principal Axis of an Airplane," NACA TN 3084, April 1954.